

FASTER Recurrent Networks for Video Classification

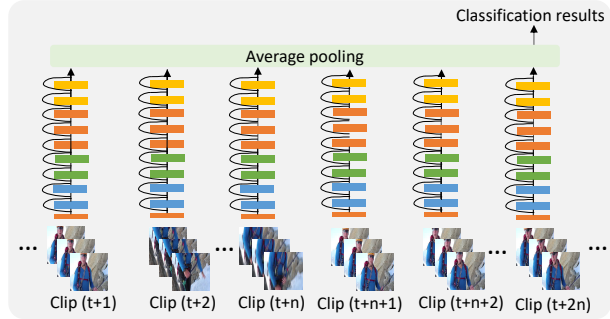
Linchao Zhu ^{†§} Laura Sevilla-Lara ^{†*} Du Tran[†] Matt Feiszli[†] Yi Yang[§] Heng Wang[†]
[†]Facebook AI [§]University of Technology Sydney ^{*}University of Edinburgh

Abstract

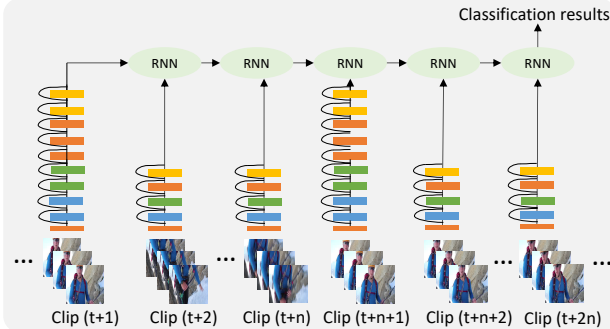
Video classification methods often divide the video into short clips, do inference on these clips independently, and then aggregate these predictions to generate the final classification result. Treating these highly-correlated clips as independent both ignores the temporal structure of the signal and carries a large computational cost: the model must process each clip from scratch. To reduce this cost, recent efforts have focused on designing more efficient clip-level network architectures. Less attention, however, has been paid to the overall framework, including how to benefit from correlations between neighboring clips and improving the aggregation strategy itself. In this paper we leverage the correlation between adjacent video clips to address the problem of computational cost efficiency in video classification at the aggregation stage. More specifically, given a clip feature representation, the problem of computing next clip’s representation becomes much easier. We propose a novel recurrent architecture called FASTER for video-level classification, that combines high quality, expensive representations of clips, that capture the action in detail, and lightweight representations, which capture scene changes in the video and avoid redundant computation. We also propose a novel processing unit to learn integration of clip-level representations, as well as their temporal structure. We call this unit FAST-GRU, as it is based on the Gated Recurrent Unit (GRU). The proposed framework achieves significantly better FLOPs vs. accuracy trade-off at inference time. Compared to existing approaches, our proposed framework reduces the FLOPs by more than 10 \times while maintaining similar accuracy across popular datasets, such as Kinetics, UCF101 and HMDB51.

1. Introduction

Video classification has made tremendous progress since the popularity of deep learning. However, while the accuracy of convolutional neural networks (CNNs) [26] on standard video datasets continues to improve, their computational cost is soaring. For example, on the popular Kinetics dataset [21], the pioneering C3D [41] reported a top-1 accu-



(a) Traditional video classification framework for inference.



(b) Our proposed framework that can process up to 75% of the clips using a much cheaper model without decreasing accuracy.

Figure 1: Traditional aggregation framework vs. proposed framework. Traditional video classification framework evaluates a single expensive network on a sequence of sampled clips. Our hybrid framework exploits the combination of expensive and cheap networks for better FLOPs/accuracy trade-offs. As adjacent clips are visually similar, computational cost can be saved by processing most of clips with a lightweight network.

racy of 63.4% with a single-clip FLOPs of 38.5G. The recent I3D [4] model improved the accuracy to an impressive 72.1% while its FLOPs also increased to 108G. Non-local networks [48] established the current state-of-the-art 77.7% accuracy on Kinetics with FLOPs as high as 359G. Moreover, this accuracy is achieved by sampling 30 clips from each video, which increases the computational cost by a

factor of 30 at test time. Though modern architectures have achieved incredible accuracy for action recognition, their high computational costs prohibit them from being widely used for real-world applications such as video surveillance, or to be deployed on hardware with limited computation power, like mobile devices.

Figure 1 (a) illustrates the traditional framework for video classification. Multiple clips are sampled from a video, and input to a computationally expensive network to generate a prediction for each clip. Clip-level predictions are then aggregated, often by taking the average, to form the final video-level prediction. To reduce the computational cost, recent efforts have focused on designing more efficient architectures [17] at the clip level. However, less attention has been paid to the efficiency of the overall framework, including how to aggregate the clip-level predictions over time, since they have such a strong temporal structure.

In this work we address the problem of reducing the computational cost of video classification by focusing on the temporal aggregation stage. In particular, we leverage the observation that video data has a strong temporal structure and is highly redundant in time. We argue that it is very computationally inefficient to process parts of the video close in time with an expensive video model, and that instead this temporal redundancy presents an opportunity to save computational costs. For this we propose a novel framework for video classification that we call *FASTER* for Feature Aggregation for Spatio-TEmporal Redundancy, and is depicted in Fig. 1 (b). Instead of processing every clip with an expensive video model, *FASTER* uses a combination of an expensive model that captures the details of the action, and a lightweight model, which captures scene changes over time, avoids redundant computation, and provides a global coverage of the entire video at a low cost. As our experimental results show in Sec. 5, up to 75% of clips can be processed with the lightweight model without affecting the classification accuracy. We also propose a novel recurrent network unit to learn temporal structure and feature aggregation over time. We call this unit *FAST-GRU*, since it is based on the Gated Recurrent Unit [7] (GRU). We observe that *FAST-GRU* is capable of learning integration of features over longer periods of time than any previous recurrent network. This is specially impressive since in our case features come from two different distributions, the expensive and the lightweight model. As a result, the *FASTER* framework achieves a significantly better FLOPs *vs.* accuracy trade-off for video classification. While maintaining the state-of-the-art accuracy across popular video datasets, its FLOPs is more than 10x smaller compared to non-local networks [48]. Code and trained models will be made publicly available at the time of publication.

In summary, we make two contributions in this paper. First, we present a new framework called *FASTER* to lever-

age temporal redundancy, and reduce FLOPs. We show that up to 75% of the clips can be processed with a much cheaper model without losing classification accuracy, maintaining state-of-the-art with 10x less FLOPs. Second, we propose a novel RNN architecture called *FAST-GRU* for the problem of learning to aggregate features over time, which is capable of learning temporal structure of features from multiple distributions, for longer periods of time than previous architectures.

The rest of the paper is organized as follows. In Sec. 2, we review related work. We then give an overview of the problem of leveraging temporal redundancy for video classification in Sec. 3, and describe the research questions that are involved in the design of the framework. We also describe the experimental details in Sec. 3, introducing the backbone architectures, training procedures, and datasets. We then dive into the first research problem in Sec. 4, which is learning to aggregate temporal information. For this, we formulate the problem, propose existing baselines, and upper and lower bounds. We perform experimental comparisons of our proposed novel *FAST-GRU* architecture to existing approaches. In Sec. 5, we explore questions regarding parameter analysis and best practices, such as the optimal proportion of lightweight and expensive models, the number and length of clips, etc. We finally compare with the state-of-the-art methods in Kinetics, UCF101 and HMDB51 in Sec. 6 and conclude the paper in Sec. 7.

2. Related Work

Early video classification approaches before the deep learning era used hand-crafted features as input to a classification method [44, 45, 25, 22, 8]. The success of CNNs in image understanding [23, 35, 33, 28], has been useful for various video understanding tasks, including action recognition [34], action detection [53], video captioning [43, 52], and video prediction [12]. In this section, we focus on the work that is most closely related to ours, which is on video classification.

Clip-level Video Classification. Much of the research efforts in video classification are focused on the problem of clip-level classification. Some of the earlier methods [34] use architectures that are largely inspired by image recognition networks [35], and operate on frames independently. In order to also learn temporal information, several works [3, 19, 20, 41] introduce the use of 3D convolutions. While this family of methods tends to produce high accuracy results, it also dramatically increases computational cost. Recent progress includes factorizing the 3D convolution into 2D spatial convolution and 1D temporal convolution [38, 32, 42, 51, 57], and designing new building blocks to learn global information on top of the 3D convolution [48, 6, 49]. Another line of research to learn temporal

information utilizes optical flow as input and designs two-stream networks [34] that use both RGB and optical flow as input to two parallel networks, or stream. After the seminal work of Simonyan *et al.*, there much effort has been devoted to improving the two-stream network [47, 55, 4, 11, 51]. A very popular example in this space is I3D [4], which adapts the Inception-V1 architecture [40], inflating 2D filters to 3D to leverage ImageNet for pre-training. Though two-stream networks often significantly improve the accuracy in practice, the usage of optical flow also increases the computational cost as accurate optical flow algorithms are expensive.

Video-level Aggregation over Time. To aggregate the predictions from the clip-level networks, average pooling is among the most popular approaches and works remarkably well in practice [34]. Besides average pooling, Karpathy *et al.* [20] proposed convolutional temporal fusion networks to aggregate the output of clip-level predictions. NetVLAD [2] has also been used [13, 30] for feature pooling on videos. Ng *et al.* [55] learned a global video representation by max-pooling over the last convolutional layer. Wang *et al.* [47] proposed the TSN network that divides the video into segments, which are averaged for classification. Zhou *et al.* [56] used a relation network to model the temporal relations between frames. Recurrent Neural Networks (RNNs) have also been adopted for sequential learning in video classification. Ng *et al.* [55] compared LSTM [16] with “Conv pooling” on UCF-101 [36], and Srivastava *et al.* [37] used LSTMs for unsupervised video feature learning. Wang *et al.* [50] proposed a spatio-temporal LSTM to extract and memorize spatial and temporal representations for video prediction. In contrast with existing work, our FAST-GRU architecture aggregates the outputs of multiple models, which further leverages spatio-temporal information for better video classification.

Efficient Networks for Video Classification. Recent work [54, 1] has also tried to reduce the computational cost of video classification by reducing the number of frames that are input to the network, using reinforcement learning. Liu *et al.* [27] used optical flow to propagate convolutional features to the following frames for object detection in video. Zolfaghari *et al.* [58] proposed the ECO model for online video understanding, where a 3D network is used to aggregate frame-level features. Our framework is orthogonal to these approaches, and it is the first to learn a combination of expensive and lightweight features.

3. Overview of FASTER

The proposed FASTER framework of Fig. 1b is a general framework to combine expensive and lightweight representations of clips over time. This generic framework contains multiple moving pieces, and designing each of these pieces

Layers	R2D-26	R(2+1)D-50	Output sizes $L \times H \times W$
conv ₁	$8 \times 7 \times 7, 64$ stride 8, 2, 2	$1 \times 7 \times 7, 45$, stride 1, 2, 2 $3 \times 1 \times 1, 64$, stride 1, 1, 1	$R2D : \frac{L}{8} \times 112 \times 112$ $R(2+1)D : L \times 112 \times 112$
pool ₁		$1 \times 3 \times 3$ max stride 1, 2, 2	$R2D : \frac{L}{8} \times 56 \times 56$ $R(2+1)D : L \times 56 \times 56$
res ₂	$\begin{bmatrix} 1 \times 1 \times 1, 64 \\ 1 \times 3 \times 3, 64 \\ 1 \times 1 \times 1, 256 \end{bmatrix} \times 2$	$1 \times 1 \times 1, 64$ $1 \times 3 \times 3, 144$ $3 \times 1 \times 1, 64$ $1 \times 1 \times 1, 256$	$R2D : \frac{L}{8} \times 56 \times 56$ $R(2+1)D : L \times 56 \times 56$
res ₃	$\begin{bmatrix} 1 \times 1 \times 1, 128 \\ 1 \times 3 \times 3, 128 \\ 1 \times 1 \times 1, 512 \end{bmatrix} \times 2$	$1 \times 1 \times 1, 128$ $1 \times 3 \times 3, 288$ $3 \times 1 \times 1, 128$ $1 \times 1 \times 1, 512$	$R2D : \frac{L}{8} \times 28 \times 28$ $R(2+1)D : \frac{L}{2} \times 28 \times 28$
res ₄	$\begin{bmatrix} 1 \times 1 \times 1, 256 \\ 1 \times 3 \times 3, 256 \\ 1 \times 1 \times 1, 1024 \end{bmatrix} \times 2$	$1 \times 1 \times 1, 256$ $1 \times 3 \times 3, 576$ $3 \times 1 \times 1, 256$ $1 \times 1 \times 1, 1024$	$R2D : \frac{L}{8} \times 14 \times 14$ $R(2+1)D : \frac{L}{4} \times 14 \times 14$
res ₅	$\begin{bmatrix} 1 \times 1 \times 1, 512 \\ 1 \times 3 \times 3, 512 \\ 1 \times 1 \times 1, 2048 \end{bmatrix} \times 2$	$1 \times 1 \times 1, 512$ $1 \times 3 \times 3, 1152$ $3 \times 1 \times 1, 512$ $1 \times 1 \times 1, 2048$	$R2D : \frac{L}{8} \times 7 \times 7$ $R(2+1)D : \frac{L}{8} \times 7 \times 7$
		spatio-temporal average pooling, fc	

Table 1: **Description of backbone architectures for the computationally expensive and lightweight model.** The number of FLOPs of R(2+1)D-50 is about $10 \times$ of R2D-26.

poses a research question, which we explore in the following. First, we ask what is the best way to learn how to aggregate features over time, and capture the temporal information inherent in video data. For this, we experiment with multiple recurrent networks, and propose a novel one, called FAST-GRU, which alleviates some of the issues in the existing networks. Second, we ask what is the optimal choice of several parameters of the framework, such as proportion of expensive and lightweight models, length of the clips and number of clips. All these parameters affect accuracy and computational cost, and here we explore the optimal balance for each of them. Finally, we analyze other smaller design choices as part of an ablation study. In the end, we provide the final FASTER framework that achieves state-of-the-art results, and 10 times faster than previous work.

Since our analyses are experimental, we start by describing the experimental setup common to all experiments, (*e.g.*, core backbone architectures for expensive and lightweight models, the datasets, and training and testing procedures). Then, in the following sections, we study and answer each of the research questions.

Backbone Architectures. Since the FASTER framework does not make any assumptions about the underlying models, we can potentially choose any of the top-performing recent networks, such as I3D [4], R(2+1)D [42] or non-local network [48]. We choose the R(2+1)D because it is one of the state-of-the-art methods, and its Github repository¹ provides a family of networks that can be used as the expensive and lightweight models.

In particular, we choose the R(2+1)D with 50 layers as expensive model, and make two changes as detailed in Ta-

¹<https://github.com/facebookresearch/VMZ>

ble 1. First we replace convolutional blocks with bottleneck layers, which has been widely used in the family of ResNet [15] architectures and shown to both reduce computational cost and improve accuracy. Second, we insert a max-pooling layer after conv_1 , which enables the R(2+1)D to support a spatial resolution of 224×224 without significantly increasing its FLOPs. Note that the input resolution to the original R(2+1)D is 112×112 . These detailed design choices further boost the performance of the network. We choose the frame-based model R2D from [42] as the lightweight model. The bottleneck layers are used in the same way as R(2+1)D. To reduce the FLOPs of R2D, a temporal stride of 8 is used in conv_1 , which effectively reduces the temporal length of the clip by a factor of 8. Unlike R(2+1)D, R2D only has 26 layers to further reduce the computational cost.

Datasets. We choose the Kinetics [21] dataset as the major testbed for our new framework. Kinetics is among the most popular datasets for video classification and it is large enough to train large models from scratch. To simplify, all experiments on our own networks that are reported on Kinetics are obtained by training from scratch, without pre-training on other video datasets (e.g., Sports1M [20]) or image datasets (e.g., ImageNet [9])². The Kinetics dataset was collected from YouTube, and has 400 action classes and about 240K training videos. We report the top-1 accuracy on the validation set as the ground truth on the testing set is not public available. To compare with the state-of-the-art, we also report results on UCF101 [36] and HMDB51 [24]. These datasets are smaller, thus we use Kinetics for pre-training and report the mean accuracy on the three testing splits.

Experimental Setup. We follow the experimental procedure of Tran *et al.* [42], since we are using their family of methods. The backbone architectures are trained with synchronous distributed SGD on GPU clusters. We make two small changes to the training setup. First, as R(2+1)D now supports a spatial resolution of 224×224 , we scale the input video whose shorter side is randomly sampled in [256, 320] pixels, following [48, 35]. Second, instead of reducing the learning rate by a factor of 10 after a number of iterations, we adopt the cosine learning rate schedule [29]. During training, we randomly sample L consecutive frames from a given video. For testing, we uniformly sample clips to cover the whole video. We fix the total number of frames to 256 frames. As the average length of Kinetics videos is about 10 seconds in 30 FPS, 256 frames gives us enough coverage over the whole video. The improvement by sampling more frames is usually marginal on Kinetics [42]. We only consider using RGB frames as the input to the model to

²Note that results reported on other papers may use pre-training, in which case we explicitly mention it.

avoid the additional computational cost introduced by using optical flow.

4. Learning to Aggregate over Time

In this section we investigate how to learn the temporal structure of clips, and aggregate diverse representations over time. We first formulate the problem of learning to aggregate, and introduce the existing baselines and our proposed FAST-GRU architecture for aggregation. We show experimental results where the FAST-GRU architecture achieves superior results, and is able to integrate information over a longer period of time.

Problem Formulation. Given a sequence of n clips from a video, we denote their feature representations as \mathbf{x}_t , where $t \in [0 \dots n - 1]$. The problem of learning to aggregate can be formulated as:

$$\mathbf{o}_t = f(\mathbf{o}_{t-1}, \mathbf{x}_t), t \in [1 \dots n - 1], \quad (1)$$

where \mathbf{o}_{t-1} encodes the historical information before the current clip. Note that Eq. 1 is exactly a recurrent neural network. One advantage of this formulation is that it does not need to cache all previous features \mathbf{x}_t unlike the widely used average pooling. Thus the framework is suitable for the online video understanding setting, applicable to live video streams, provides classification results at any time, and overall takes us one step close to end-to-end video classification. This framework does not make assumptions about the feature tensor \mathbf{x}_t . In our experiments, we use the feature map from the last convolutional layer, which is a tensor of shape $l \times h \times w \times c$, as shown in Fig. 2. Once the features are aggregated, they are fed to a fully-connected layer, which will output the classification result.

Baselines. Many successful methods have learned to aggregate temporal information over time, in the context of video classification. Here we choose the most widely used, as well as the most related to our FAST-GRU.

Mixed average pooling is the most naïve baseline, and consists of all clip-level predictions being averaged together. While this choice may seem too simple, it is surprisingly effective, and it is the prevailing one. In the *concat* baseline, features \mathbf{x}_t and \mathbf{o}_{t-1} are concatenated together, and then projected to a joint feature space, as in Fig. 2a. More formally, the *concat* model is computed as

$$f(\mathbf{o}_{t-1}, \mathbf{x}_t) = \text{ReLU}(\text{BN}(\mathbf{W}\mathbf{o}_{t-1} + \mathbf{U}\mathbf{x}_t)), \quad (2)$$

where weight matrices \mathbf{W} and \mathbf{U} are learnable variables shared across time steps. We include batch normalization [18] and ReLU [31] activation, as they are considered best practices to make the baseline stronger. Recurrent networks such as LSTM [16] and GRU [7] are the most closely related baselines. These are the go-to methods for tasks that

involve temporal modeling [39], such as language or audio. They use a gating mechanism to integrate new input and historical information, or possibly to forget the learned history. For the LSTM baseline, we use the variant that consists of three gates and an additional cell between time steps [14]. LSTM has a forget gate that can reset the history to the current input. In some tasks, *e.g.*, machine translation, this forget gate helps refresh the state when a new sentence starts. In the video domain this may be helpful in the case of different camera shots or unrelated actions. GRU is another popular RNN, which introduces two gates, *i.e.*, the read gate and the update gate. The state transition function uses the update gate to perform a weighted average of the historical state and the current internal representation.

FAST-GRU. In the traditional RNN setting, input features are often 1D vectors computed by average pool. While this representation is lightweight, it also completely eliminates spatial information, which is useful in the case of video understanding. Instead of using a fully-connected layer to process the flattened convolutional features, we keep the original shape of the features, and use a $1 \times 1 \times 1$ convolution for feature projection. We perform global spatio-temporal pooling on the output of FAST-GRU to do the final classification. We empirically show that spatio-temporal information is beneficial for long sequence modeling, which has been largely ignored in recent video pooling methods based on recurrent networks.

The gating mechanism is one of the key components in RNNs, and enables useful functionality for temporal sequence modeling. Conditioned on the historical information, the importance of the next input is decided by a subnetwork. The subnetwork learns to combine the state and the input with the gating mechanism. Here, we build on the traditional gating function by adding a bottleneck structure that increases expressiveness, both because it compresses the input and because it introduces an additional non-linearity. In the original GRU architecture, the subnetwork is the concatenation of \mathbf{x}_t and \mathbf{o}_{t-1} , projected to a vector of the original size c . Specifically, the two gates are computed by

$$\begin{aligned} \mathbf{r}_t &= \sigma(\mathbf{G}_{rx}\mathbf{x}_t + \mathbf{G}_{ro}\mathbf{o}_{t-1}), \\ \mathbf{z}_t &= \sigma(\mathbf{G}_{zx}\mathbf{x}_t + \mathbf{G}_{zo}\mathbf{o}_{t-1}), \end{aligned} \quad (3)$$

where \mathbf{G}_* are matrices of $c \times c$, and σ is the sigmoid function. In FAST-GRU, we aim to enforce more information to be encoded with a bottleneck layer. The information between the history and the current input will be integrated in a smaller feature space. Specifically, the dimensionality of the channel is first reduced by r with a $1 \times 1 \times 1$ convolutional layer. After that, there is a ReLU followed by a $1 \times 1 \times 1$ convolution increasing the channel dimensionality to the original size c . The read gate and the update gate are

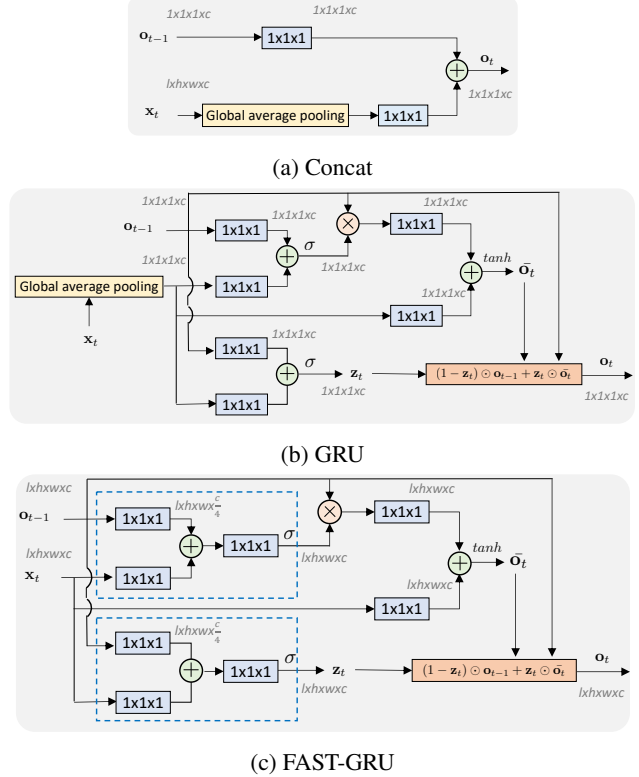


Figure 2: **Different architectures to learn temporal structure.** The “Concat” baseline can learn pairwise information for short periods of time. The GRU can learn longer sequences, but saturates. The FAST-GRU architecture leverages spatio-temporal information, and is capable of representing information over longer sequences. The bottleneck structure (in dash rectangle) in the gate function reduces computational cost and improves gating capabilities.

computed as

$$\begin{aligned} \mathbf{r}'_t &= \text{ReLU}(\mathbf{U}_{rx} * \mathbf{x}_t + \mathbf{U}_{ro} * \mathbf{o}_{t-1}), \\ \mathbf{z}'_t &= \text{ReLU}(\mathbf{U}_{zx} * \mathbf{x}_t + \mathbf{U}_{zo} * \mathbf{o}_{t-1}), \\ \mathbf{r}_t &= \sigma(\mathbf{W}_{r'} * \mathbf{r}'_t), \\ \mathbf{z}_t &= \sigma(\mathbf{W}_{z'} * \mathbf{z}'_t), \end{aligned} \quad (4)$$

where \mathbf{U}_* are $1 \times 1 \times 1$ convolutions to reduce the channel size by a ratio of r , and \mathbf{W}_* are $1 \times 1 \times 1$ convolutions to increase the channel size to c . Our gate is generated by taking the joint compressed feature \mathbf{r}'_t and \mathbf{z}'_t , which enables more powerful gating for feature aggregation. This bottleneck layer also reduces the computational cost by r . We empirically set r to be 4, as it performs best in our preliminary experiments. After the calculation of \mathbf{r}_t and \mathbf{z}_t , The output of FAST-GRU (Fig. 2c) is

$$\begin{aligned} \bar{\mathbf{o}}_t &= \tanh(\mathbf{V}_{\bar{o}} * \mathbf{x}_t + \mathbf{V}_{\bar{o}} * (\mathbf{r}_t \odot \mathbf{o}_{t-1})), \\ \mathbf{o}_t &= (1 - \mathbf{z}_t) \odot \mathbf{o}_{t-1} + \mathbf{z}_t \odot \bar{\mathbf{o}}_t, \end{aligned} \quad (5)$$

where \mathbf{V}_* are trainable variables.

Experimental setup. We compare the accuracy of the baselines across a wide range of number of clips ($n = \{2, 4, 8, 16, 32\}$), keeping 1 expensive and $n-1$ cheap clips, all of length $L = 8$ frames. This allows us to observe the behavior of different architectures in shorter and longer sequences. The initial state \mathbf{o}_0 is initialized with the features of the first clip. We train the network over 7 epochs³, where the first 2 are warm-up and the learning rate is cosine-decayed for the remaining 5. At training time clips are sampled in order, but at random distances, as a form of temporal data augmentation. At test time, clips are sampled to be equidistant.

Comparison of RNNs. The results are shown in Table 2. We observe that the performance of the “Avg. pool (mixed)” baseline saturates as more cheap clips are added. Less accurate predictions dominate the final score, since the accuracy of the cheap model using 16 clips is 64.0%, quite similar to the “Avg. pool (mixed)” with 32 clips, which achieves 63.8%. This suggests that the expensive features are not fully utilized. “Concat” outperforms “Avg. pool (mixed)” by 2.1% when $n = 8$, showing the benefits of learning temporal structure. However, as n increases, the performance of “Concat” decreases, and by $n = 32$, the accuracy is 8.1% lower than $n = 8$. This shows that the learning to aggregate over a longer time period is difficult. Interestingly, “Concat”, and all recurrent networks have similar performances when the number of clips is small, $n = 2, 4$, showing that the advantage of RNNs is not evident for short sequences. As the number of clips increases ($n \geq 16$), recurrent methods show their strength in modeling long sequences and perform better than “Concat”. As the number of clips increases, performance drops 1.6% in the case of LSTMs.

Of all methods, FAST-GRU achieves best performance for long sequences. For example, FAST-GRU outperforms GRU by 1.4% when $n = 32$, and by 1.3% when $n = 16$. The results show our proposed FAST-GRU is beneficial for long sequence learning, even when sequence samples come from different distributions.

FASTER vs. Prevailing Average Pooling. How well does the FASTER framework do with respect to the prevailing average pooling? Recall that our main focus is not only to increase accuracy, but to reduce computational cost. For this, we plot the GFLOPs vs. accuracy in Fig. 3. We compare FASTER to the traditional framework where all clips are cheap (or all clips are expensive) and integrated with average pooling. These are the lower and upper bound respectively of the proposed framework. There is a 7% gap between the top performance of the cheap and the expensive network. However, this comes at a 10 \times increase in the cost.

³Follow [42], the size of one epoch is set to 1,000,000.

Model	Number of Clips				
	2	4	8	16	32
Avg. pool (mixed)	60.7	63.9	64.2	64.0	63.8
Concat	61.6	65.9	66.3	62.3	58.2
LSTM	61.3	66.2	66.3	66.3	64.7
GRU	61.1	65.6	66.5	66.1	65.8
FAST-GRU	61.1	65.6	67.2	67.4	67.2

Table 2: **Comparison of aggregation architectures with varying number of input clips on Kinetics.** Note that all methods use the same features, *i.e.*, only the first clip is processed by the expensive model, and the rest of the clips by the lightweight model.

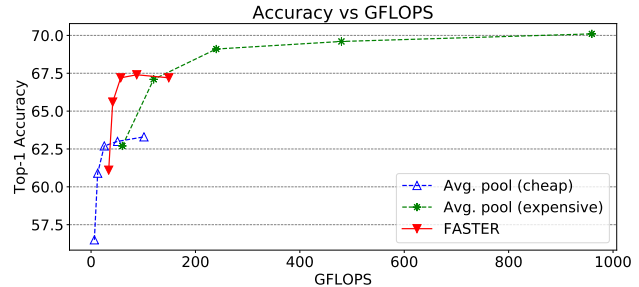


Figure 3: **FASTER vs. traditional frameworks with average pooling.** We show accuracy vs. GFLOPs of different as a function of the number of clips. We compare the results of FAST-GRU from Table 2 with average pooling of all expensive (Avg. pool (expensive)) and lightweight model (Avg. pool (cheap)). FASTER brings in the best of both worlds.

Our proposed FASTER brings in the best of both worlds. FASTER saves 40% computational cost while obtains 3.9% gains in accuracy. When $n = 4$, it takes 119 GFLOPs for “Avg. pool (expensive)” to achieve 67.1%. FASTER can achieve comparable results with half the cost.

Note that there is still an accuracy gap between FASTER and “Avg. pool (expensive)”. In the next section, we study the optimal combination of input features and actually achieve results superior to using only expensive features.

5. FASTER Best Practices

In the previous section we have focused on the design of the FASTER framework for a fixed parameter setting, and have observed that it produces better results than previous work. We now go one step further and explore how to achieve the best trade-off in practice. For this we first analyze the behavior of the framework when varying different parameters, such as length of clips, number of clips and proportion of expensive models and cheap models. We also explore the benefit of adding spatial convolutional pooling at test time, confirming the effectiveness of keeping spatio-temporal information until the classification layer.

#E : #C	8-fr \times 32-clips		16-fr \times 16-clips		32-fr \times 8-clips	
	V@1	GFLOPs	V@1	GFLOPs	V@1	GFLOPs
All E (A)	70.1	959.4	72.3	959.4	74.5	959.3
All E (F)	70.6	982.4	72.9	980.2	74.9	979.2
1:1	70.5	553.6	72.9	552.0	74.6	550.4
1:3	70.1	339.2	72.1	337.6	73.3	336.0
1:7	69.6	230.4	71.7	230.4	71.3	228.8
1:15	69.0	176.0	69.9	176.0		
1:31	67.2	150.4				

Table 3: **Many short clips or few long clips?** For a fixed number of total frames we vary number of clips and clip size, and measure accuracy and GFLOPs on Kinetics. Empty cells correspond to combinations that are not feasible. “E” denotes the expensive model, while “C” denotes the cheap model. Baselines “All E (A)” and “All E (F)” refer to using all expensive models aggregated via average pooling and via our FAST-GRU respectively. GFLOPs combine the cheap, expensive and FAST-GRU models together.

Parameter Analysis. There are three parameters in our framework that affect accuracy and computational cost: length of the clip (L) in frames, number of clips (n), and the proportion of expensive and lightweight clips used as input pattern. In this section we provide an empirical study of these parameters to achieve the best trade-off. Since we are interested in the behavior of the network, we “fix” the input data by keeping the number of frames constant at 256, which spans the entire video. Thus, $L \times n = 256$ for all settings. Given n clips, we experiment with input patterns of $1+x$, where $x \in \{1, 3, 7, 15, 31\}$. Additionally, we evaluate the case where all the inputs are expensive features ($x = 0$). Results are shown in Table 3.

As it is expected, a higher ratio of expensive models leads to higher accuracy. For example, when $L = 8$, there is a large gap of 1.8% when x goes from 31 to 15, with a modest increase of 25.6 GFLOPs. The gap is less obvious for higher ratios of expensive models.

A remarkable observation is that when $x = 3$, FASTER achieves 70.1% which is the same as the average pooling baseline with all expensive model, while only takes 35% of its GFLOPs. Even more, for $x = 1$, the proposed method outperforms the average pooling baseline, at 57% of the cost. This shows the benefit of learning temporal aggregation of hybrid inputs.

We also observe that for a fixed cost, it is often beneficial to use larger clip size L . For example, for a fixed proportion of cheap models $x = 3$, the accuracy of the 32-fr \times 8-clips is higher than 16-fr \times 16-clips, and that in turn considerably higher than the 8-fr \times 32-clips. In other words, it is better to have fewer clips with more frames. However, for higher ratios of cheap clips (*e.g.*, $x = 7$), the pattern does not hold.

We choose the parameter setting $L = 16$ and $x = 7$ as

	FASTER16		FASTER32	
	V@1	GFLOPs	V@1	GFLOPs
w/o spatial conv-pool	71.7	230.4	74.6	550.4
with spatial conv-pool	72.2	300.6	75.1	719.0

Table 4: **Spatial convolutional pooling results.** We observe that spatial convolutional pooling improves results on FASTER models, at some additional computational cost.

the best inexpensive configuration, and call it FASTER16. It indicates that it is possible to achieve better performance with lower L , which reflects the importance of learning a good aggregation function. When $L = 32$ and $x = 1$, the proposed framework achieves 74.6% accuracy with 550.4 GFLOPs. We denote this model as FASTER32 and it is the best model when the cost is around \sim 550 GFLOPs.

Finally, FASTER also works when all input features come from the same network. When the inputs are all expensive features, FASTER outperforms the average pooling baseline in all settings, for an additional $1.02\times$ the cost.

Spatial Convolutional Pooling. We evaluate the effectiveness of spatial convolutional pooling to validate the importance of maintaining spatio-temporal information across all time steps. At the inference time, instead of cropping a 224×224 patch from the frame, we take the 256×256 patch. Thus, more spatial information will be captured both in the convolutional layers and the recurrent layers. We evaluate spatial convolutional pooling on the FASTER16 and FASTER32 models. The results are shown in Table 4. Note that spatial convolutional pooling has been attempted before [4], however, they did not observe improvements when using a larger patch. Since our framework uses more spatial information, the accuracy of FASTER16 and FASTER32 improves by 0.5%, at $1.3\times$ the cost.

6. Comparison to state-of-the-art

We now compare our proposed framework to state-of-the-art methods across three of the most popular video classification datasets, *i.e.*, Kinetics, UCF-101 and HMDB-51. We include methods that use RGB frames as inputs. Numerical results on Kinetics are shown in Table 5. These same numbers are also visualized in terms of accuracy *vs.* GFLOPs in Figure 4. Our proposed FASTER framework achieves the best accuracy *vs.* GFLOPs trade-off of all methods. FASTER32 outperforms its own building block R(2+1)D-34 by 3.1% with its 4% GFLOPs. FASTER16 outperforms I3D trained from scratch by 3.8% (72.2% *vs.* 68.4%), using only 70% of I3D’s cost (432 GFLOPs). As can be seen, pre-training on ImageNet boosts the performance a lot. For example, I3D is improved by 3.7% when enables ImageNet pre-training, and S3D is improved by 3.8% as well. As we focus on the design of the frame-

Model	Top-1	Pretrain	GFLOPs \times crops
I3D [4]	72.1	ImageNet	108 \times 4
S3D [51]	72.2	ImageNet	66.4 \times N/A
MF-Net [6]	72.8	ImageNet	11.1 \times 50
A^2 -Net [5]	74.6	ImageNet	40.8 \times 30
S3D-G [51]	74.7	ImageNet	71.4 \times N/A
NL I3D-50 [48]	76.5	ImageNet	282 \times 30
NL I3D-101 [48]	77.7	ImageNet	359 \times 30
I3D [4]	68.4	-	108 \times 4
STC [10]	68.7	-	N/A \times N/A
ARTNet [46]	69.2	-	23.5 \times 250
S3D [51]	69.4	-	66.4 \times N/A
ECO [58]	70.0	-	N/A \times N/A
R(2+1)D-34 [42]	72.0	-	152 \times 115
FASTER16 w/o sp	71.7	-	14.4 \times 16
FASTER32	75.1	-	89.9 \times 8

Table 5: **Comparisons to state-of-the-art methods on Kinetics.** Inputs are RGB frames. Top-1 accuracy is reported. For “GFLOPs \times crops”, we report the cost of a single crop and the numbers of crops used. “N/A” indicates the crops are not reported in the paper.

	Pretrain	UCF-101	HMDB-51
STC [10]	Kinetics	95.8	72.6
ARTNet [46]	Kinetics	94.3	70.9
ECO [58]	Kinetics	93.6	68.4
R(2+1)D-34 [42]	Kinetics	96.8	74.5
I3D [4]	ImageNet+Kinetics	95.6	74.8
S3D [51]	ImageNet+Kinetics	96.8	75.9
FASTER32	Kinetics	96.9	75.7

Table 6: **Comparisons to state-of-the-art methods on UCF-101 and HMDB-51.**

work, the benefits of pre-training on other datasets like ImageNet [9] and Sports-1M [20] should be transferable to our framework. Even though we do not leverage pre-training, our framework outperforms all existing pre-trained models except NL-I3D. However, FASTER32 uses 6% of the GFLOPs of NL-I3D. Our FASTER32 model outperforms A^2 -Net by 0.5%, while the cost is reduced by 42%. The results validate the effectiveness of our FASTER framework, showing it is promising to leverage the combination expensive and lightweight models for better FLOPs vs. accuracy trade-off.

Competitive results are also achieved on UCF-101 and HMDB-51 datasets as shown in Table 6. It shows learning the aggregation function on larger dataset can facilitate the generalization on smaller datasets. The improvements are less profound as the performance on small datasets tends to be saturated.

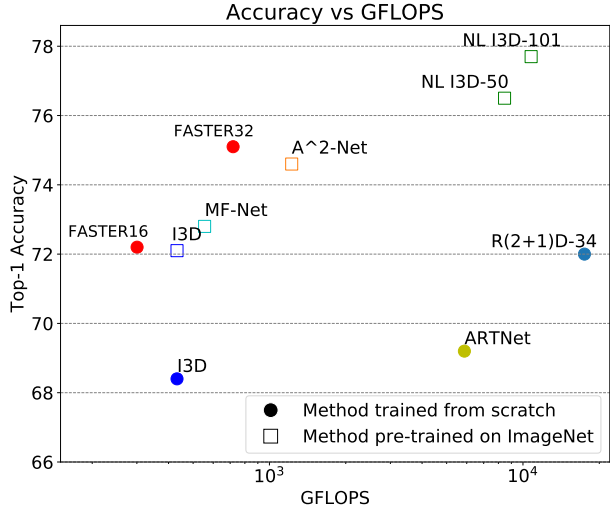


Figure 4: **Log-scale Accuracy vs. GFLOPs comparisons for state-of-the-art methods on Kinetics.** In this chart, optimal methods are closer to the top-left corner. The two proposed variants of FASTER are the closest to the corner. This is specially impressive since they are not pre-trained on ImageNet, and since they build on backbone architectures that are not particularly cost effective. For example, the FASTER16 setting achieves similar accuracy to R(2+1)D, and it is two orders of magnitude cheaper. Overall, the FASTER framework provides the best cost vs. accuracy trade-off of all methods.

7. Conclusion

In this paper, we propose a novel framework called FASTER for efficient video classification. To exploit the temporal redundancy, we use a combination of expensive and lightweight features. Learning to aggregate over time these diverse features is a difficult problem and thus we propose a recurrent unit called FAST-GRU for aggregating mixed features. We conduct sufficient analysis to study the portion of expensive and lightweight models, the effect of using different clip lengths, and the effectiveness of maintaining spatial information. The resulting FASTER framework saves 24 \times the cost of its building block R(2+1)D-34, while still outperforms it by 3.1%. In the future, we will study more dynamic sampling strategies that could learn to adapt and select the clips for expensive feature extraction according to the content of the video.

References

- [1] H. Alwassel, F. Caba Heilbron, and B. Ghanem. Action search: Spotting actions in videos and its application to temporal action localization. In *ECCV*, 2018. 3
- [2] R. Arandjelovic, P. Gronat, A. Torii, T. Pajdla, and J. Sivic. Netvlad: Cnn architecture for weakly supervised place

- recognition. In *Proceedings of the IEEE Conference on Computer Vision and Pattern Recognition*, pages 5297–5307, 2016. 3
- [3] M. Baccouche, F. Mamalet, C. Wolf, C. Garcia, and A. Baskurt. Sequential deep learning for human action recognition. In *International Workshop on Human Behavior Understanding*, 2011. 2
- [4] J. Carreira and A. Zisserman. Quo vadis, action recognition? a new model and the kinetics dataset. In *CVPR*, 2017. 1, 3, 7, 8
- [5] Y. Chen, Y. Kalantidis, J. Li, S. Yan, and J. Feng. A²-nets: Double attention networks. In *NIPS*, pages 350–359, 2018. 8
- [6] Y. Chen, Y. Kalantidis, J. Li, S. Yan, and J. Feng. Multi-fiber networks for video recognition. In *ECCV*, 2018. 2, 8
- [7] K. Cho, B. van Merriënboer, C. Gulcehre, F. Bougares, H. Schwenk, and Y. Bengio. Learning phrase representations using RNN encoder-decoder for statistical machine translation. In *EMNLP*, 2015. 2, 4
- [8] N. Dalal, B. Triggs, and C. Schmid. Human detection using oriented histograms of flow and appearance. In *ECCV*, 2006. 2
- [9] J. Deng, W. Dong, R. Socher, L.-J. Li, K. Li, and L. Fei-Fei. ImageNet: A Large-Scale Hierarchical Image Database. In *CVPR09*, 2009. 4, 8
- [10] A. Diba, M. Fayyaz, V. Sharma, M. M. Arzani, R. Yousefzadeh, J. Gall, and L. Van Gool. Spatio-temporal channel correlation networks for action classification. In *ECCV*, 2018. 8
- [11] C. Feichtenhofer, A. Pinz, and A. Zisserman. Convolutional two-stream network fusion for video action recognition. In *CVPR*, 2016. 3
- [12] C. Finn, I. Goodfellow, and S. Levine. Unsupervised learning for physical interaction through video prediction. In *NIPS*, 2016. 2
- [13] R. Girdhar, D. Ramanan, A. Gupta, J. Sivic, and B. Russell. Actionvlad: Learning spatio-temporal aggregation for action classification. In *CVPR*, 2017. 3
- [14] A. Graves. Generating sequences with recurrent neural networks. *arXiv preprint arXiv:1308.0850*, 2013. 5
- [15] K. He, X. Zhang, S. Ren, and J. Sun. Deep residual learning for image recognition. In *CVPR*, 2016. 4
- [16] S. Hochreiter and J. Schmidhuber. Long short-term memory. *Neural Computation*, 9(8):1735–1780, 1997. 3, 4
- [17] A. G. Howard, M. Zhu, B. Chen, D. Kalenichenko, W. Wang, T. Weyand, M. Andreetto, and H. Adam. Mobilenets: Efficient convolutional neural networks for mobile vision applications. *arXiv preprint arXiv:1704.04861*, 2017. 2
- [18] S. Ioffe and C. Szegedy. Batch normalization: Accelerating deep network training by reducing internal covariate shift. In *ICML*, 2015. 4
- [19] S. Ji, W. Xu, M. Yang, and K. Yu. 3d convolutional neural networks for human action recognition. *TPAMI*, 2013. 2
- [20] A. Karpathy, G. Toderici, S. Shetty, T. Leung, R. Sukthankar, and L. Fei-Fei. Large-scale video classification with convolutional neural networks. In *CVPR*, 2014. 2, 3, 4, 8
- [21] W. Kay, J. Carreira, K. Simonyan, B. Zhang, C. Hillier, S. Vijayanarasimhan, F. Viola, T. Green, T. Back, P. Natsev, et al. The kinetics human action video dataset. *arXiv preprint arXiv:1705.06950*, 2017. 1, 4
- [22] A. Klaser, M. Marszałek, and C. Schmid. A spatio-temporal descriptor based on 3d-gradients. In *BMVC*, 2008. 2
- [23] A. Krizhevsky, I. Sutskever, and G. E. Hinton. ImageNet classification with deep convolutional neural networks. In *NIPS*, 2012. 2
- [24] H. Kuehne, H. Jhuang, E. Garrote, T. Poggio, and T. Serre. Hmdb: a large video database for human motion recognition. In *ICCV*, 2011. 4
- [25] I. Laptev. On space-time interest points. *IJCV*, 2005. 2
- [26] Y. LeCun, L. Bottou, Y. Bengio, and P. Haffner. Gradient-based learning applied to document recognition. *Proceedings of the IEEE*, 86(11):2278–2324, 1998. 1
- [27] M. Liu and M. Zhu. Mobile video object detection with temporally-aware feature maps. In *CVPR*, 2018. 3
- [28] W. Liu, D. Anguelov, D. Erhan, C. Szegedy, S. Reed, C.-Y. Fu, and A. C. Berg. Ssd: Single shot multibox detector. In *ECCV*, 2016. 2
- [29] I. Loshchilov and F. Hutter. Sgdr: Stochastic gradient descent with warm restarts. *arXiv preprint arXiv:1608.03983*, 2016. 4
- [30] A. Miech, I. Laptev, and J. Sivic. Learnable pooling with context gating for video classification. *arXiv preprint arXiv:1706.06905*, 2017. 3
- [31] V. Nair and G. E. Hinton. Rectified linear units improve restricted boltzmann machines. In *ICML*, 2010. 4
- [32] Z. Qiu, T. Yao, and T. Mei. Learning spatio-temporal representation with pseudo-3d residual networks. In *ICCV*, 2017. 2
- [33] S. Ren, K. He, R. Girshick, and J. Sun. Faster r-cnn: Towards real-time object detection with region proposal networks. In *NIPS*, 2015. 2
- [34] K. Simonyan and A. Zisserman. Two-stream convolutional networks for action recognition in videos. In *NIPS*, 2014. 2, 3
- [35] K. Simonyan and A. Zisserman. Very deep convolutional networks for large-scale image recognition. In *ICLR*, 2015. 2, 4
- [36] K. Soomro, A. R. Zamir, and M. Shah. UCF101: A dataset of 101 human actions classes from videos in the wild. *arXiv preprint arXiv:1212.0402*, 2012. 3, 4
- [37] N. Srivastava, E. Mansimov, and R. Salakhudinov. Unsupervised learning of video representations using LSTMs. In *ICML*, 2015. 3
- [38] L. Sun, K. Jia, D.-Y. Yeung, and B. E. Shi. Human action recognition using factorized spatio-temporal convolutional networks. In *ICCV*, 2015. 2
- [39] I. Sutskever, O. Vinyals, and Q. V. Le. Sequence to sequence learning with neural networks. In *NIPS*, 2014. 5
- [40] C. Szegedy, W. Liu, Y. Jia, P. Sermanet, S. Reed, D. Anguelov, D. Erhan, V. Vanhoucke, and A. Rabinovich. Going deeper with convolutions. In *CVPR*, 2015. 3
- [41] D. Tran, L. Bourdev, R. Fergus, L. Torresani, and M. Paluri. Learning spatiotemporal features with 3D convolutional networks. In *ICCV*, 2015. 1, 2

- [42] D. Tran, H. Wang, L. Torresani, J. Ray, Y. LeCun, and M. Paluri. A closer look at spatiotemporal convolutions for action recognition. In *CVPR*, 2018. [2](#), [3](#), [4](#), [6](#), [8](#)
- [43] S. Venugopalan, M. Rohrbach, J. Donahue, R. Mooney, T. Darrell, and K. Saenko. Sequence to sequence-video to text. In *ICCV*, 2015. [2](#)
- [44] H. Wang, A. Kläser, C. Schmid, and C.-L. Liu. Action recognition by dense trajectories. In *CVPR*, 2011. [2](#)
- [45] H. Wang and C. Schmid. Action recognition with improved trajectories. In *ICCV*, 2013. [2](#)
- [46] L. Wang, W. Li, W. Li, and L. Van Gool. Appearance-and-relation networks for video classification. In *CVPR*, 2017. [8](#)
- [47] L. Wang, Y. Xiong, Z. Wang, Y. Qiao, D. Lin, X. Tang, and L. Van Gool. Temporal segment networks: Towards good practices for deep action recognition. In *ECCV*, 2016. [3](#)
- [48] X. Wang, R. Girshick, A. Gupta, and K. He. Non-local neural networks. In *CVPR*, 2018. [1](#), [2](#), [3](#), [4](#), [8](#)
- [49] X. Wang and A. Gupta. Videos as space-time region graphs. In *ECCV*, 2018. [2](#)
- [50] Y. Wang, M. Long, J. Wang, Z. Gao, and S. Y. Philip. Predrnn: Recurrent neural networks for predictive learning using spatiotemporal lstms. In *NIPS*, 2017. [3](#)
- [51] S. Xie, C. Sun, J. Huang, Z. Tu, and K. Murphy. Rethinking spatiotemporal feature learning: Speed-accuracy trade-offs in video classification. In *ECCV*, 2018. [2](#), [3](#), [8](#)
- [52] L. Yao, A. Torabi, K. Cho, N. Ballas, C. Pal, H. Larochelle, and A. Courville. Describing videos by exploiting temporal structure. In *ICCV*, 2015. [2](#)
- [53] S. Yeung, O. Russakovsky, N. Jin, M. Andriluka, G. Mori, and L. Fei-Fei. Every moment counts: Dense detailed labeling of actions in complex videos. *IJCV*, 2018. [2](#)
- [54] S. Yeung, O. Russakovsky, G. Mori, and L. Fei-Fei. End-to-end learning of action detection from frame glimpses in videos. In *CVPR*, 2016. [3](#)
- [55] J. Yue-Hei Ng, M. Hausknecht, S. Vijayanarasimhan, O. Vinyals, R. Monga, and G. Toderici. Beyond short snippets: Deep networks for video classification. In *CVPR*, 2015. [3](#)
- [56] B. Zhou, A. Andonian, A. Oliva, and A. Torralba. Temporal relational reasoning in videos. In *ECCV*, 2018. [3](#)
- [57] Y. Zhou, X. Sun, Z.-J. Zha, and W. Zeng. Mict: Mixed 3d/2d convolutional tube for human action recognition. In *CVPR*, 2018. [2](#)
- [58] M. Zolfaghari, K. Singh, and T. Brox. Eco: Efficient convolutional network for online video understanding. In *ECCV*, 2018. [3](#), [8](#)